View metadata, citation and similar papers at core.ac.uk
brought to you by CORE
provided by Digital Repository @ Iowa State University

ANALYSIS OF ACOUSTIC EMISSION OUTPUT FROM PROPAGATING FATIGUE CRACK

I. M. Daniel, C. G. Sifniotopoulos and J.-J. Luo

Robert R. McCormick School of Engineering and Applied Science
Northwestern University
Evanston, IL 60208

INTRODUCTION

Acoustic emission (AE) is a very useful approach in detecting and characterizing fatigue damage growth in general and crack initiation and propagation in particular. Numerous studies have been conducted dealing with correlations of AE output and fracture mechanics and fatigue damage parameters [1-9]. It has been shown that under monotonic loading AE can detect yielding and that the cumulative AE output from a notched specimen is directly related to the stress intensity factor [10]. However, such correlations between AE and damage may not be easy to establish because of the influence of loading, material, geometric and noise factors. In application of the AE method, discrimination between signal and noise is of paramount importance.

The objective of this study was to investigate and analyze the acoustic emission output from a propagating crack in a metallic notched specimen under fatigue loading. The investigation consisted of signal/noise discrimination, direct crack growth monitoring, acquisition and processing of AE data, and correlation of AE data with damage growth.

EXPERIMENTAL PROCEDURE

The material investigated was 4340 steel. The specimen type used was a standard compact tension specimen (ASTM E399, Fig. 1). The specimens had overall dimensions of 9.53 cm (3.75 in.) by 9.14 cm (3.60 in.) and a thickness of 12.7 mm (0.5 in.). A crack of initial length a_0 = 30.5 mm (1.2 in.) was machined by EDM prior to heat treatment. The crack had a 60° V-shaped tip and a crack tip radius of 0.102 mm (0.004 in.).

Two 150 kHz resonance transducers (R15, Physical Acoustics) were placed at equal distances from the source (notch). The AE data were acquired and processed by a digital multichannel system (MISTRAS 2001, Physical Acoustics). Crack extension during fatigue testing was monitored using crack propagation gages as shown in Fig. 1. Two such gages were mounted ahead of the initial crack, a higher resolution gage near the initial crack tip in order to better pinpoint crack initiation and the first stage of crack propagation and a coarser gage farther down the expected crack path (TK-09-CPA01-005/DP and TK-09-CPC03-003/DP, Measurements Group).

As anticipated, signal/noise discrimination was identified as the most crucial problem. Various methods of noise suppression were considered. High-pass frequency filtering can filter out low frequency noise. Threshold filtering can suppress all lower amplitude noise. However, there may still be some higher frequency and higher amplitude noise reaching the transducers. Spatial filtering techniques based on guard sensors or differential time of arrival can be used to eliminate noise from external sources away from

Review of Progress in Quantitative Nondestructive Evaluation, Vol 17
Edited by D.O. Thompson and D.E. Chimenti, Plenum Press, New York, 1998

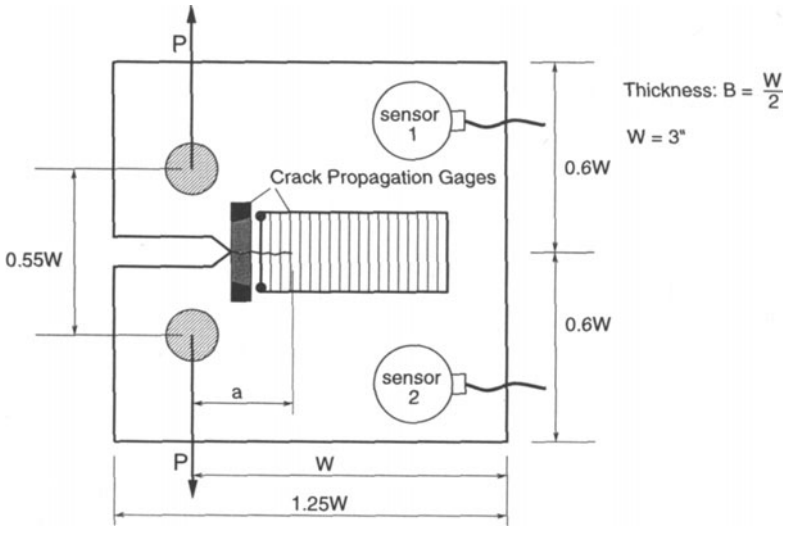

Figure 1. Compact tension specimen with AE sensors and crack propagation gages. (ASTM E399).

the notch. Noise can also be separated by analyzing the individual waveforms and identifying special characteristics attributed to noise. The method of noise suppression used was threshold filtering and spatial filtering based on the differential time of arrival [11]. Signals emanating from the source would arrive at the two sensors nearly simultaneously. Signals (noise) from external sources, such as one end of the specimen, would arrive at the sensors at times differing by approximately $\Delta t = s/c$, where c = wave speed and s = distance between transducers. Only signals with a difference in time of arrival of $\Delta t < s/c$ need to be retained. This type of filtering can be performed automatically by the instrumentation system used. In the present case $s/c \cong 19$ μs, but only signals with a time difference of $\Delta t < 2$μs were retained.

Fatigue tests were conducted in a servohydraulic testing machine at a stress ratio R = 0.1, and at a cyclic frequency of 2 Hz. During data acquisition, preamplifiers with 40 dB gain were used and a threshold of 34-37 dB was set. A number of fatigue tests were conducted at various initial peak stress intensity factors K_{max} ranging from $K_{max} = 0.15\ K_{Ic}$ to $K_{max} = 0.35\ K_{Ic}$ where K_{Ic} is the critical stress intensity factor of the material.

RESULTS

The normalized cumulative number of AE counts and the crack length are plotted versus normalized fatigue cycles for four different tests conducted at two different peak loads (Fig. 2). All four AE plots display jumps, mostly in the first half of the fatigue life, whereas the crack length increases smoothly. The jumps for higher K_{max} occur earlier than those for the lower K_{max}. Furthermore, the crack extension curve plotted versus normalized fatigue cycles is identical in all four cases and appears to be independent of loading amplitude. This apparently unexpected result is explained below.

The stress intensity factor for the specimen geometry of Fig. 1 is given by

$$K_I = \frac{P}{B\sqrt{W}} f(\alpha) \qquad (1)$$

where

$$\alpha = \frac{a}{W}$$

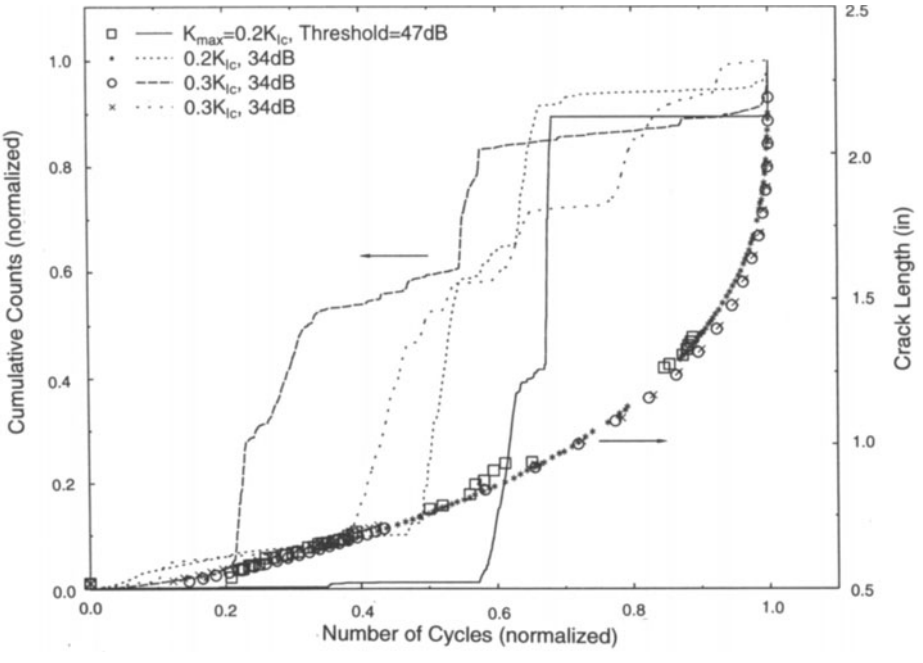

Figure 2. Normalized cumulative AE counts and crack length vs. normalized number of fatigue cycles for four 4340 steel specimens.

and

$$f(\alpha) = \frac{(2+\alpha)\left(0.886 + 4.64\,\alpha - 13.32\alpha^2 + 14.72\alpha^3 - 5.6\alpha^4\right)}{(1-\alpha)^{3/2}}$$

The stress intensity factor range ΔK during fatigue is given by

$$\Delta K = \frac{\Delta P}{B\sqrt{W}}\, f(\alpha) \tag{2}$$

Crack length results from various tests were plotted versus ΔK on log-log scale from which the crack growth rate per fatigue cycle, da/dn was obtained and plotted versus ΔK (Fig. 3). The results of the various tests can be described for the most part by the Paris relation

$$\frac{da}{dn} = C(\Delta K_I)^m \tag{3}$$

which, in view of eq. (2) yields

$$\frac{d\alpha}{[f(\alpha)]^m} = \frac{C}{W}\left(\frac{\Delta P}{B\sqrt{W}}\right)^m dn \tag{4}$$

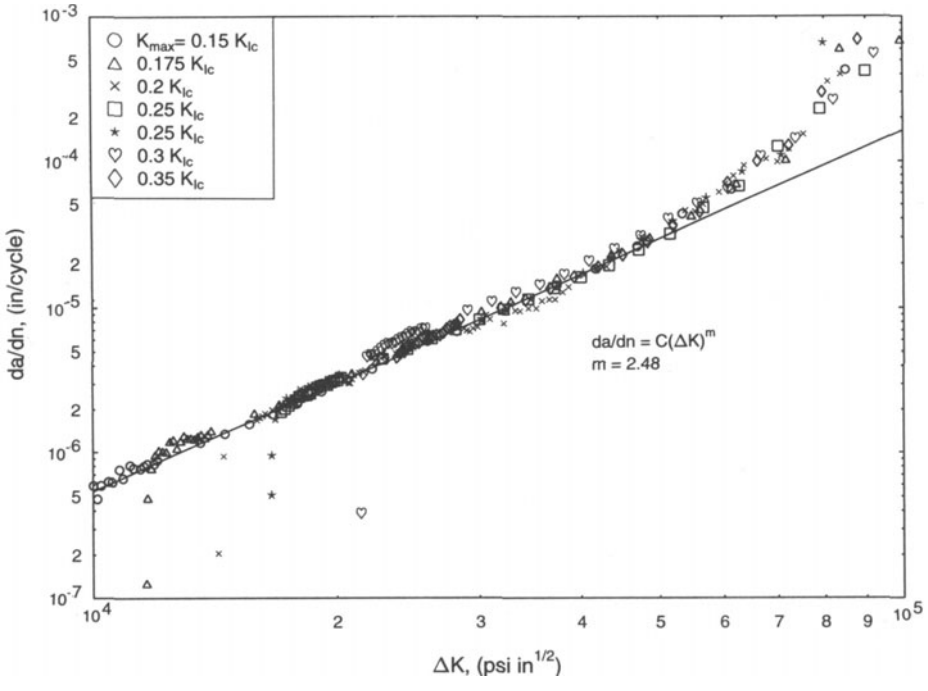

Figure 3. Crack growth rate vs. ΔK for various K_{max} amplitudes.

and, by integration from the initial condition (a_0, n_0) to the current one (a, n),

$$\frac{C}{W}\left(\frac{\Delta P}{B\sqrt{W}}\right)^m (n - n_0) = F(\alpha) - F(\alpha_0) \tag{5}$$

where

$$F(\alpha) = \int_0^{\alpha} \frac{d\alpha}{[f(\alpha)]^m} \tag{6}$$

At failure $a = a_f$ and $n = n_f$ and eq. (5) yields

$$\frac{n - n_0}{n_f - n_0} = \frac{F(\alpha) - F(\alpha_0)}{F(\alpha_f) - F(\alpha_0)} \tag{7}$$

The functions $f(\alpha)$ and $F(\alpha)$ are plotted versus the variable $\alpha = a/W$ in Fig. 4. It is seen from this plot that when $\alpha_f > 0.5$ for this case

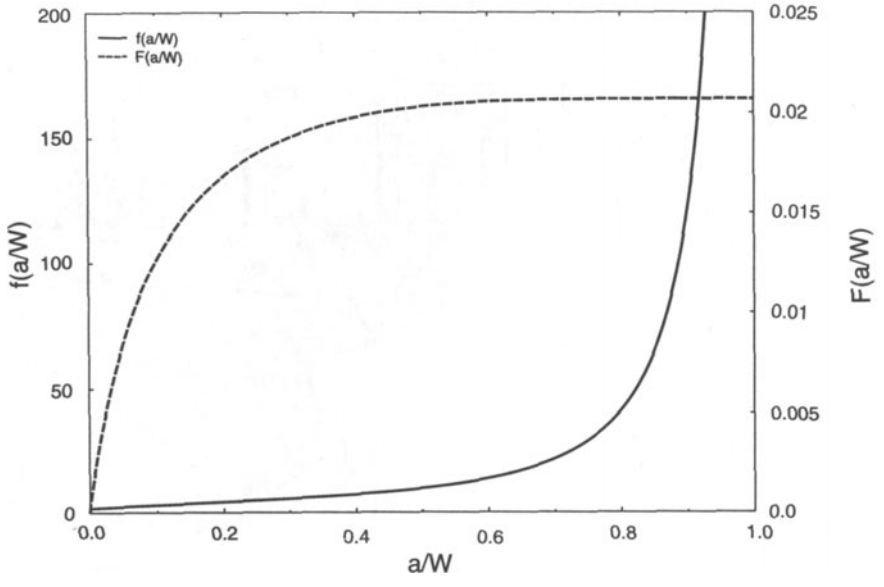

Figure 4. Plot of functions f (a/W) and F(a/W) for compact tension specimen. (Paris exponent m = 2.48)

$$F(\alpha_f) \cong F(1) = F_m = \text{constant}$$

$$F_m = \int_0^1 \frac{d\alpha}{[f(\alpha)]^m} \tag{8}$$

If $n_0 = 0$, eq. (7) takes the form

$$\frac{n}{n_f} \cong \frac{F(\alpha) - F(\alpha_0)}{F_m - F(\alpha_0)} \tag{9}$$

or $$\alpha = G(\alpha_0, m, n/n_f) \tag{10}$$

The last equation shows that, for a wide range of loads corresponding to $\alpha_f > 0.5$, the crack length is a function of normalized fatigue life and independent of loading amplitude as observed in Fig. 2.

It was observed that AE activity occurs at all levels and phases of the loading cycle, both during loading ($\varphi < 180°$) and during unloading ($\varphi > 180°$). A typical cumulative AE curve is shown in Fig. 5 divided into six ranges or stages along with the corresponding loading phase distribution of the AE activity. This distribution of AE activity is also represented graphically in Fig. 6. It is seen that the AE output can be separated into three groups or regions according to the phase of the loading cycle at which it occurs. AE signals in group A occur throughout the fatigue lifetime and correspond to the end of the unloading cycle ($\varphi > 250°$). AE signals in group B occur during the loading part of the cycle at a phase angle φ decreasing with fatigue cycles. AE signals in group C occur near the end of the fatigue lifetime near the peak of the loading cycle. Although the AE activity appears to be widely distributed, the majority of the AE counts belong in group B.

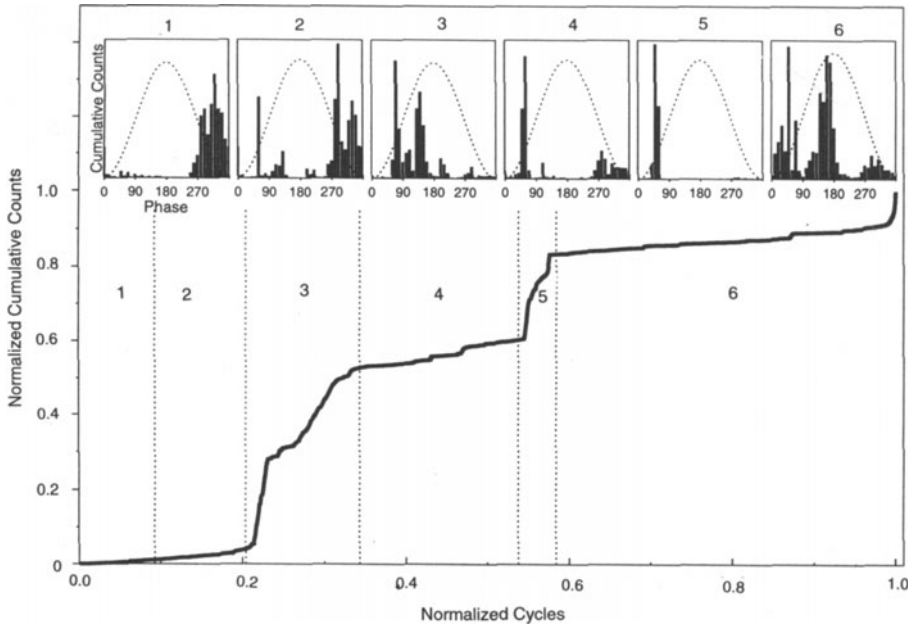

Figure 5. Cumulative AE counts and corresponding loading phase distributions at several stages (4340 steel; compact tension specimen).

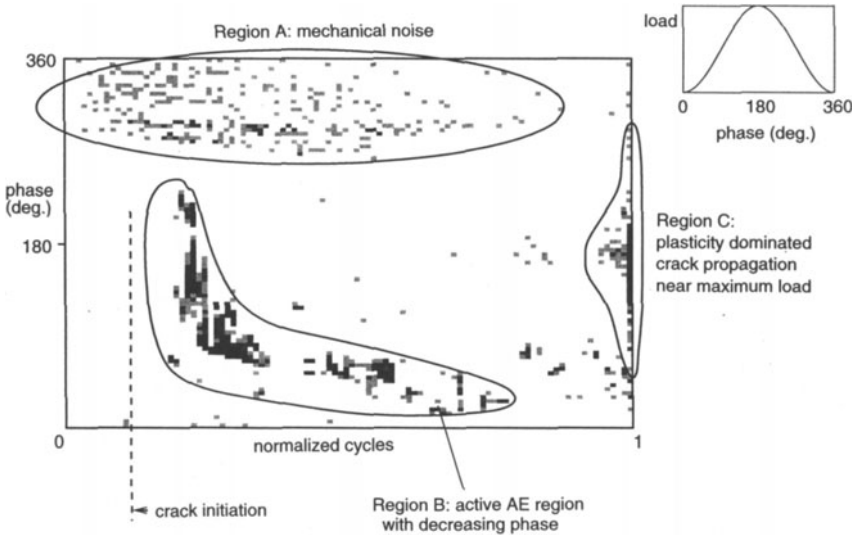

Figure 6. Loading phase distribution and grouping of AE activity (4340 steel; compact tension specimen).

The origin of AE signals of the various groups was investigated by plotting the differential time of arrival (Δt) distribution of AE hits (Fig. 7). The wide Δt distribution of group A is an indication that signals in this group are caused by noise. Signals of group B seem to be concentrated within a narrow range ($\pm$ 2 μs) of differential time of arrival, therefore, their likely source is the crack opening and propagation. Signals in group C also are for the most part concentrated in a narrow range of differential time of arrival Δt, and are attributed to rapid crack propagation in the final stage of the fatigue life.

The signal groups above were also examined in terms of the amplitude distribution of the duration (Fig. 8). AE hits in group A are randomly distributed over a short duration/short amplitude region, as would be the case for noise AE hits of group B show a linear relation between duration and amplitude, a fact that implies an exponentially damped signal. Hits in group show a similar linear variation, therefore are equally attributable to an exponentially damped signal coming from a propagating crack.

SUMMARY AND CONCLUSIONS

Techniques were developed for monitoring of AE activity during cyclic loading of notched metallic specimens. The material studied was 4340 steel and the specimen type used was a standard compact tension specimen. The AE output was monitored with a pair of resonant transducers equally spaced from the specimen notch. Crack propagation was monitored independently and concurrently with AE output.

Crack growth was found to be a function of normalized fatigue lifetime but independent of fatigue load amplitude for a wide range of test parameters. Whereas crack

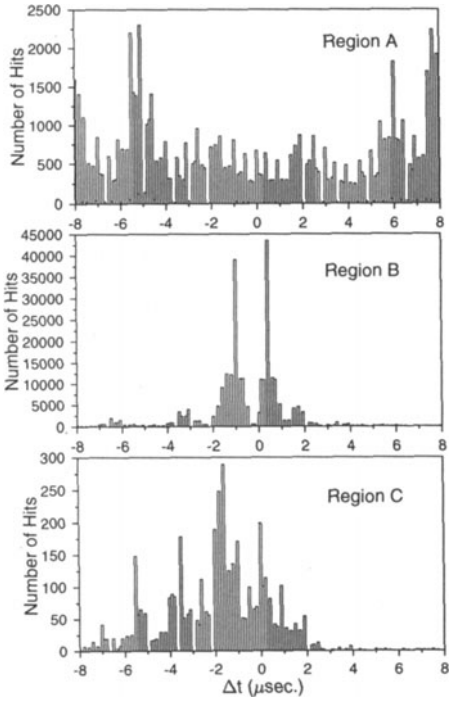

Figure 7. Differential time of arrival (Δt) distribution of AE hits (4340 steel; compact tension specimen; $K_{max} = 0.175\ K_{Ic}$).

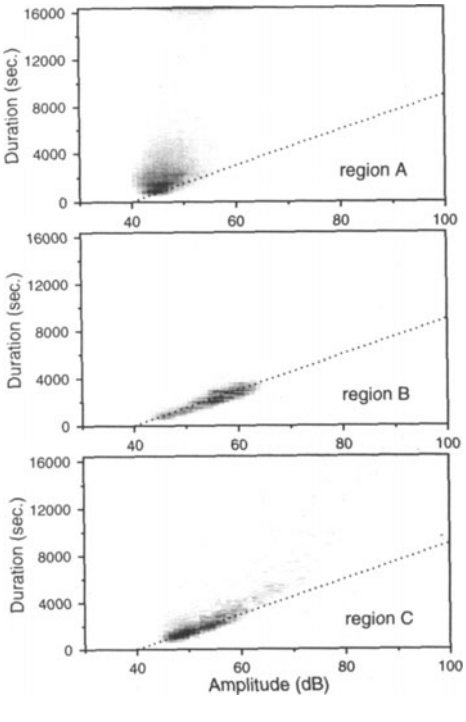

Figure 8. Amplitude distribution of AE hit durations for three groups (4340 steel; compact tension specimen; $K_{max} = 0.175\ K_{IC}$).

growth increases smoothly with fatigue cycles, AE output shows jumps near the middle of the fatigue lifetime.

The phase of the loading cycle was identified as an important parameter in analyzing AE data. The AE output can be separated into three groups or regions according to the phase of the loading cycle at which it occurs. AE signals in group A correspond to the end of the unloading cycle ($\varphi > 250°$). They are primarily associated with noise. AE signals in group B occur during the loading part of the cycle at a phase angle φ decreasing with fatigue cycles. This activity which takes the form of jumps, corresponds to crack opening and crack propagation. AE signals in group C occur near the end of the fatigue lifetime near the peak of the loading cycle. They correspond to rapid crack propagation in the final stage.

ACKNOWLEDGEMENTS

This work was sponsored by the Office of Naval Research (ONR) under a Multi-University Research Initiative (M-URI)program. We are grateful to Mrs. Yolande Mallian for typing the manuscript.

REFERENCES

1. D. Fang and A. Berkovits, "Fatigue Damage Mechanisms on the Basis of Acoustic Emission Measurements," *Novel Exper. Techniques in Fracture Mechanics*, ed. by A. Shukla, AMD-Vol. 176, ASME, 1993, pp. 213-235.
2. *Acoustic Emission Testing* in *Nondestructive Testing Handbook,* Vol. 5, ed. by R. K. Miller and P. McIntire, Second Ed., American Soc. for Nondestructive Testing, Columbus, OH, 1987.
3. H. L. Morton, R. M. Harrington and J. G. Bjeletich, "Acoustic Emission of Fatigue Crack Growth," *Engineering Fracture Mechanics*, Vol. 5, No. 3, 1973, pp. 691-697.
4. T. C. Lindley, I. G. Palmer and C. E. Richards, "Acoustic Emission Monitoring of Fatigue Crack Growth," *Materials Science and Engineering,* Vol. 32, 1978, pp. 1-15.
5. F. Hamel, J. P. Bailon and M. N. Bassim, "Acoustic Emission Mechanisms during High Cycle Fatigue," *Engin. Fracture Mech.,* Vol. 14, No. 4, 1981, pp. 853-860.
6. A. Berkovits and D. Fang, "An Empirical Design Model for Fatigue Damage on the Basis of Acoustic Emission Measurements," 17th ICAF Symposium, Stockholm, June 1993.
7. A. C. Sinclair, D. C. Connors and C. L. Formby, "Acoustic Emission Analysis during Fatigue Crack Growth in Steel," *Materials Science and Engineering,* Vol. 28, 1977, pp. 263-273.
8. D. H. Kohn, P. Ducheyne and J. Awerbuch, "Acoustic Emission during Fatigue of Ti-6Al -4V: Incipient Fatigue Crack Detection Limits and Generalized Data Analysis Methodology," *J. of Materials Science,* Vol. 27, 1992, pp. 3133-3142.
9. S. Smith and T. M. Morton, "Acoustic-Emission Detection Technique for High-Cycle-Fatigue Testing," *Exper. Mech.,* Vol. 13, 1973, pp. 193-198.
10. H. L. Dunegan and D. O. Harris, "Acoustic Emission - A New Nondestructive Testing Tool," *Ultrasonics,* Vol. 7, No. 3, 1969, pp. 160-166.
11. I. M. Daniel, J.-J. Luo, C. G. Sifniotopoulos and H.-J. Chun, "Acoustic Emission Monitoring of Fatigue Damage in Metals," *Review of Progress in QNDE,* ed. by D. O. Thompson and D. E. Chimenti, Vol. 16, Plenum Press, New York, 1997, pp. 451-458.